

Reflect3r: Single-View 3D Stereo Reconstruction Aided by Mirror Reflections

Supplementary Material

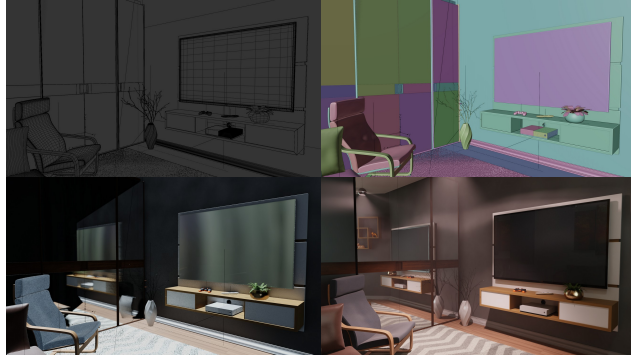


Figure 9. Details of the **synthetic** dataset’s Blender modeling. Top left: wireframe view; top right: solid view; bottom left: material view; bottom right: rendered view. The scene is fully customizable, allowing adjustments to the mirror’s position and properties, as well as the room setup and lighting, enabling easy extension of the dataset.

733

7. Implementation Details

734
735
736
737
738
739
740
741
742
743
744
745
746
747

We explain more details about the mirror plane recovery in Sec. 5.1. Since DUS3R lacks direct correspondences in the mirror region, its predicted mirror plane is often inaccurate in position, though the normal direction is generally reliable. Our objective is to recover both the plane’s normal and its position. Our goal is to obtain the normal and the position of the plane. The normal is estimated using the method described in Eq. (11). For plane positioning, we first extract edge points in the main view via image-space edge detection and back-project them into 3D. RANSAC is then applied to remove outliers. To improve robustness, we retain the top 10% of edge points ranked by DUS3R’s confidence scores and randomly select one as a reliable anchor point to finalize the plane position.

748

8. More Details About the Synthetic Data

749
750

We provide the thumbnail of all 16 scenes included in our dataset in Fig. 10.

751
752
753
754
755
756
757
758
759

Figure 9 shows an example Blender scene in our dataset. Each scene in the dataset can be fully customized, including object shapes, room layouts, furniture placement, material properties, lighting conditions, etc. We additionally insert and adjust mirror surfaces with controllable positions and reflectance properties to simulate realistic reflective setups. This design not only ensures diverse and detailed scenes for training and evaluation but also provides a flexible foundation for extending the dataset in future work.

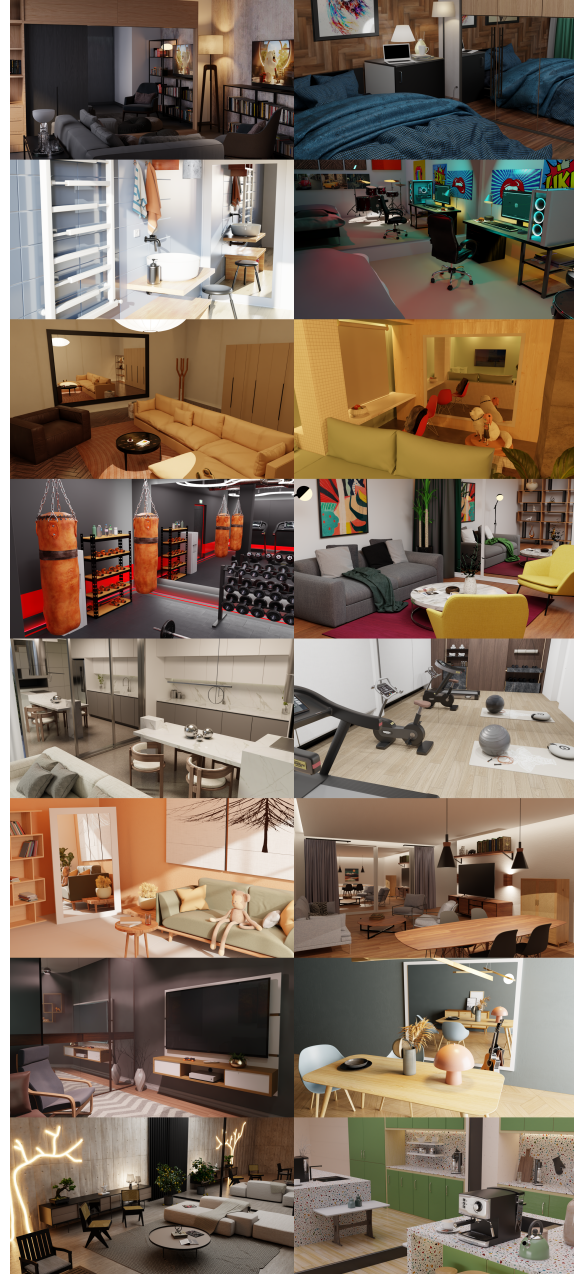


Figure 10. Thumbnails of the 16 fully editable Blender scenes included in our dataset.

9. More Details About the Experiments

9.1. Details of Evaluation Metrics

We cover the math of the evaluation metrics in this section.

Given the ground-truth point cloud $\mathcal{P} = \{\mathbf{p}_i\}_{i=1}^{N_p}$ and the reconstructed point cloud $\mathcal{Q} = \{\mathbf{q}_i\}_{i=1}^{N_q}$, Chamfer Distance

760

761

762

763

764

765 is computed as

$$766 \quad \frac{1}{2N_P} \sum_{\mathbf{p} \in \mathcal{P}} \min_{\mathbf{q} \in \mathcal{Q}} \|\mathbf{p} - \mathbf{q}\|_2 + \frac{1}{2N_Q} \sum_{\mathbf{q} \in \mathcal{Q}} \min_{\mathbf{p} \in \mathcal{P}} \|\mathbf{p} - \mathbf{q}\|_2 \quad (17)$$

767 In our paper, we report the completeness (Comp.) and
768 the accuracy (Accu.) in percentage with a threshold of 1 cm
769 of the point cloud distance. Specifically, let the indicator
770 function be $\mathbf{I}[\cdot]$,

$$771 \quad \text{Comp.} = \frac{1}{N_P} \sum_{\mathbf{p} \in \mathcal{P}} \mathbf{I}[\min_{\mathbf{q} \in \mathcal{Q}} \|\mathbf{p} - \mathbf{q}\|_2 < 1\text{cm}]; \quad (18)$$

$$772 \quad \text{Accu.} = \frac{1}{N_Q} \sum_{\mathbf{q} \in \mathcal{Q}} \mathbf{I}[\min_{\mathbf{p} \in \mathcal{P}} \|\mathbf{p} - \mathbf{q}\|_2 < 1\text{cm}]; \quad (19)$$

$$773 \quad \text{F1} = \frac{2 \cdot \text{Comp.} \cdot \text{Accu.}}{\text{Comp.} + \text{Accu.}}. \quad (20)$$

774 9.2. More Statistics And Analysis

775 To further assess robustness, we visualize the score dis-
776 tributions in Fig. 11 using boxplots for completeness, ac-
777 curacy, and F1 score on the synthetic dataset. Reflect3r
778 achieves the highest median scores across all metrics while
779 also exhibiting the smallest interquartile range and whisker
780 span, indicating low variance and strong stability across
781 scenes. MoGe attains similar median scores to Reflect3r,
782 suggesting that its predicted point clouds are close to the
783 ground-truth, but its results fluctuate significantly, reflect-
784 ing high variance. Its completeness is notably lower, as
785 MoGe does not leverage the stereo information provided
786 by mirrors and therefore fails to recover occluded regions,
787 leaving parts of the scene uncovered. DUS3R and VGGT,
788 unable to identify mirrors, generate false geometry in reflec-
789 tive regions and consequently show much higher variability.
790 MAST3R, which cannot handle single-view reconstruction,
791 consistently predicts flat geometry and therefore yields uni-
792 formly low scores.

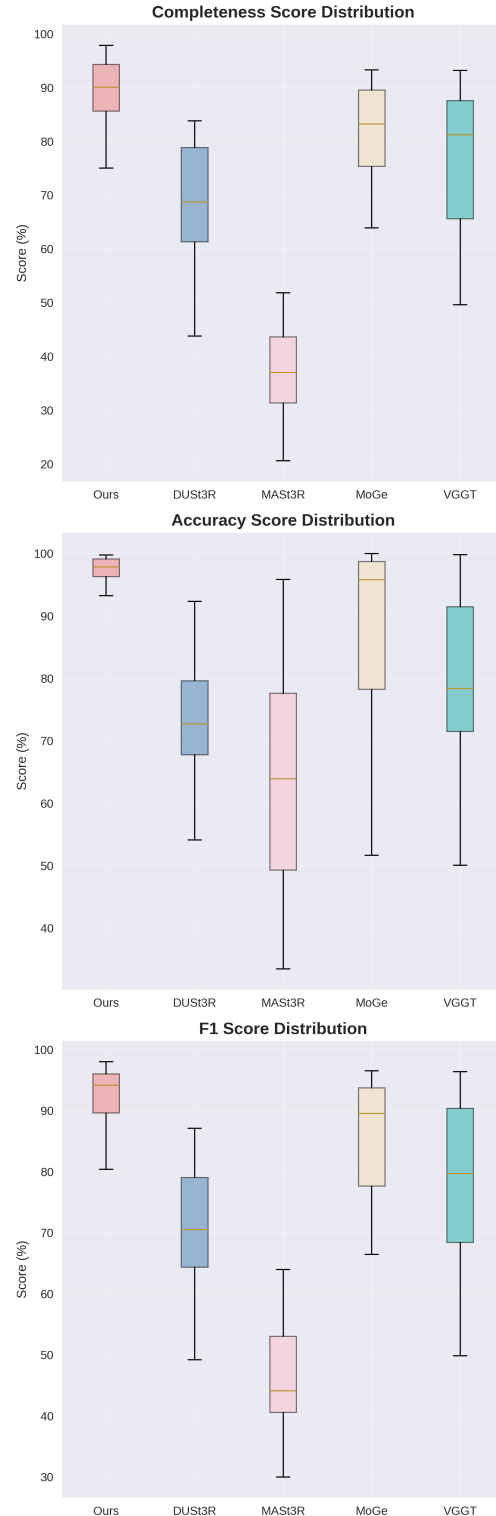


Figure 11. Boxplots of completeness, accuracy, and F1 score on the synthetic dataset.